

Article

## A Modified Surface on Titanium Deposited by a Blasting Process

Caroline O’Sullivan <sup>1,2,\*</sup>, Peter O’Hare <sup>3</sup>, Greg Byrne <sup>4</sup>, Liam O’Neill <sup>5</sup>, Katie B. Ryan <sup>1</sup> and Abina M. Crean <sup>1</sup>

<sup>1</sup> School of Pharmacy, Cavanagh Building, University College Cork, Cork, Ireland; E-Mails: katie.ryan@ucc.ie (K.B.R.); a.crean@ucc.ie (A.M.C.)

<sup>2</sup> Department of Chemical and Process Engineering, Cork Institute of Technology, Bishopstown, Cork, Ireland

<sup>3</sup> The Nanotechnology and Integrated BioEngineering Centre, University of Ulster at Jordanstown, Newtownabbey, Co Antrim, BT37 0QB, Northern Ireland; E-Mail: p.ohare@ulster.ac.uk

<sup>4</sup> School of Electrical, Electronic & Mechanical Engineering, University College Dublin, Belfield, Dublin 4, Ireland; E-Mail: gregory.byrne@ucd.ie

<sup>5</sup> Research & Development, EnBIO, Carrigtohill, Cork, Ireland; E-Mail: liam.oneill@enbiomaterials.com

\* Author to whom correspondence should be addressed; E-Mail: caroline.osullivan@cit.ie; Tel.: +353-(0)21-490-1667; Fax: +353-(0)21-490-1656.

Received: 16 July 2011; in revised form: 23 August 2011 / Accepted: 1 September 2011 /

Published: 13 September 2011

---

**Abstract:** Hydroxyapatite (HA) coating of hard tissue implants is widely employed for its biocompatible and osteoconductive properties as well as its improved mechanical properties. Plasma technology is the principal deposition process for coating HA on bioactive metals for this application. However, thermal decomposition of HA can occur during the plasma deposition process, resulting in coating variability in terms of purity, uniformity and crystallinity, which can lead to implant failure caused by aseptic loosening. In this study, CoBlast<sup>TM</sup>, a novel blasting process has been used to successfully modify a titanium (V) substrate with a HA treatment using a dopant/abrasive regime. The impact of a series of apatitic abrasives under the trade name MCD, was investigated to determine the effect of abrasive particle size on the surface properties of both microblast (abrasive only) and CoBlast (HA/abrasive) treatments. The resultant HA treated substrates were compared

to substrates treated with abrasive only (microblasted) and an untreated Ti. The HA powder, apatitic abrasives and the treated substrates were characterized for chemical composition, coating coverage, crystallinity and topography including surface roughness. The results show that the surface roughness of the HA blasted modification was affected by the particle size of the apatitic abrasives used. The CoBlast process did not alter the chemistry of the crystalline HA during deposition. Cell proliferation on the HA surface was also assessed, which demonstrated enhanced osteo-viability compared to the microblast and blank Ti. This study demonstrates the ability of the CoBlast process to deposit HA coatings with a range of surface properties onto Ti substrates. The ability of the CoBlast technology to offer diversity in modifying surface topography offers exciting new prospects in tailoring the properties of medical devices for applications ranging from dental to orthopedic settings.

**Keywords:** hydroxyapatite; grit blasting; CoBlast; hard tissue implants

---

## 1. Introduction

Hydroxyapatite (HA),  $\text{Ca}_{10}(\text{PO}_4)_6(\text{OH})_2$ , a proven bioceramic for coating medical device implants is widely known, not only for its biocompatible and osteoconductive properties, but also for its increased mechanical properties when applied to bio-inert metals for orthopedic use [1-4]. Implant surface modifications are often required in order to prescribe a particular surface roughness and increase surface area for osteoblast attachment, as well as to enhance the bioactive and osteoconductive properties of the underlying substrate. Such surface treatment methods include sand- or grit-blasting using abrasives, chemical treatments and deposition of calcium phosphate (CaP) coatings [2-8].

Abrasive blasting involves impacting the implant metal surface with abrasive particles under pressure to roughen the surface. Roughening orthopedic and dental implants utilizing alumina ( $\text{Al}_2\text{O}_3$ ) abrasives is a common practice to enhance implant osteointegration *in vivo* [5,6]. However, the use of apatite abrasives are often preferred as it enhances bone formation [7,18]. It has been shown that this technique can be effective in depositing a thin layer of CaP on the surface being roughened [18-20]. A number of other HA coating deposition techniques have been employed to confer a bioactive layer onto metallic and other inert substrates including plasma spraying, which is one of the most common types of coating process for the generation of CaP thin films [3,4,9-14] and alternative deposition processes including pulsed laser deposition (PLD) [15], radio frequency (RF) magnetron sputtering [16], sol-gel immersion techniques, and electrophoretic deposition [17].

More recently, a novel approach CoBlast has been shown as an alternative process to deposit HA and substituted apatites onto titanium (Ti) substrates [21-23]. The CoBlast technique is based on the convergent flow of an abrasive and a dopant stream onto the implant surface which can effectively impregnate the metal with the dopant material. The CoBlast approach manipulates the ability of abrasive blasting to achieve surface roughening and bioactive layer deposition. The impregnation of the dopant material onto the surface results from a combination of the mechanical interlocking and tribo-chemical bond formation between the bioceramic material and the underlying metal

substrate [21]. HA coatings prepared using the CoBlast technique demonstrated enhanced osteoblast attachment *in vitro* and early stage lamellar bone growth *in vivo* compared to microblasted and untreated Ti surfaces [21]. Additionally, a series of substituted apatites (AgA, SrA, ZnA) were effectively deposited using the CoBlast technique and these modifications offered the dual benefits of osteoconductive properties essential for bone integration with the added potential of microbial colonization inhibition without cytotoxic effects [23]. The established research showed that  $<10\ \mu\text{m}$  thick coatings were applied with this technique employing alumina as the abrasive and that there was no evidence of alumina being incorporated into the modified surface [21].

The objective of this study is to demonstrate the use of apatitic abrasives in the treatment of Ti substrates using both the CoBlast technique (dopant/abrasive regime) and a control microblast surface (abrasive only). The chemical, topological and osteo-viability advantages of treated Ti substrates was characterised. The effect of abrasive particle size on the properties and performance of the CoBlast and microblast modified surfaces was also investigated. A series of apatitic abrasives (sintered CaP under the trade name MCD) with differing mean particle size values were employed for both techniques.

## 2. Results and Discussion

### 2.1. Chemical Characterization of HA and MCD Abrasive Powders

The particle size of the HA and MCD abrasives were measured using a laser light technique (Mastersizer S), Table 1. The average particle size ( $d(0.5)$ ) increased in the following order: HA < MCD-106 < MCD-180 < MCD-425. The various powders were analyzed for their chemical composition using energy dispersive X-ray (EDX) analysis, Table 1.

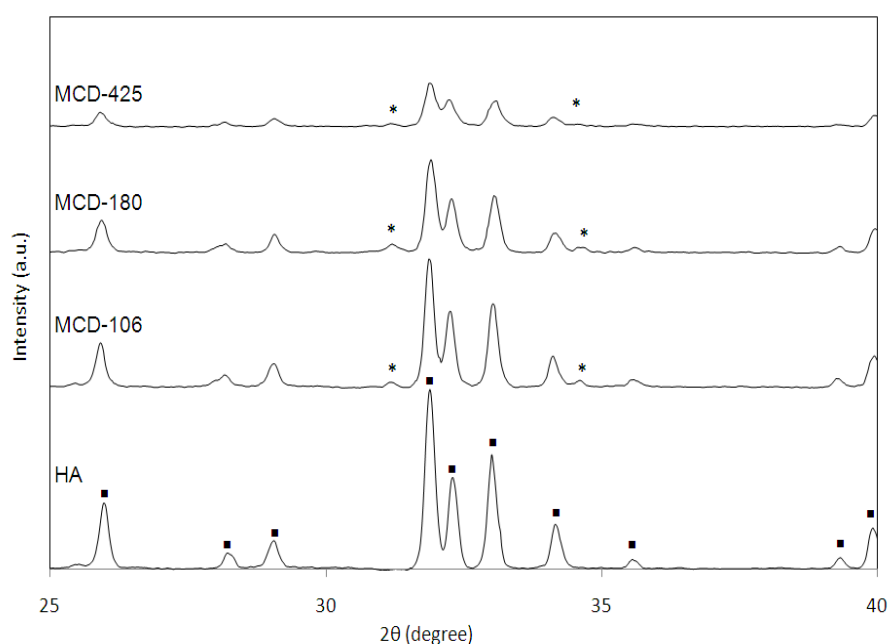
**Table 1.** Mean particle size analysis and energy dispersive X-ray (EDX) analysis of the calcium phosphate powders ( $n = 3$ ).

Powder	Mean particle Size ( $\mu\text{m}$ )	O % atm	Ca % atm	P % atm	Ca/P
HA	40 ( $\pm 4$ )	71	18	11	1.66
MCD-106	44 ( $\pm 2$ )	72	18	10	1.76
MCD-180	124 ( $\pm 6$ )	73	17	10	1.73
MCD-425	355 ( $\pm 6$ )	77	13	10	1.29

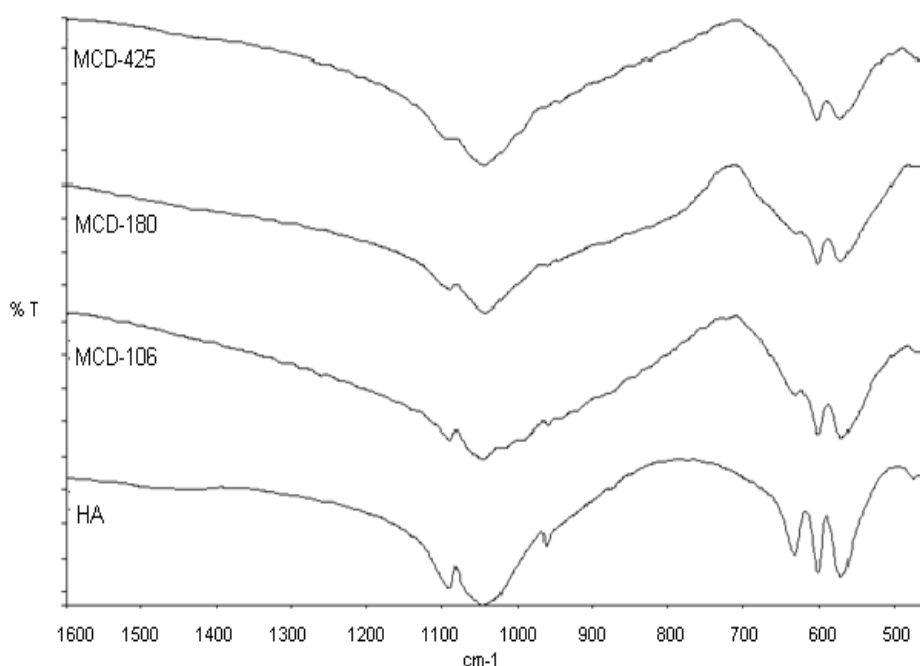
The calcium phosphate powders (HA and MCD abrasives) were found to be composed of O, P and Ca. The Ca/P ratio for stoichiometric HA was found to be similar to the previously reported value of 1.67 [25]. The increase in Ca/P ratio for MCD-106 and MCD-180, as seen in Table 1, may be explained by the presence of impurities such as tricalcium phosphate (TCP) phase as determined by powder X-ray diffraction (PXRD) analysis (Figure 1). However, the Ca deficient nature for the more amorphous MCD-425 results in a reduced Ca/P ratio (1.29).

Relative crystallinity of each powder was investigated using PXRD, (Figure 1). HA was found to be highly crystalline with well defined narrow peaks. The main characteristic peaks associated with HA can be assigned to the 002, 102, 210, 211, 112, 300 and 202 reflections corresponding to  $25.9^\circ$ ,  $28.1^\circ$ ,  $28.9^\circ$ ,  $31.9^\circ$ ,  $32.2^\circ$ ,  $33.1^\circ$  and  $34.1^\circ$ , as previously reported [25]. The resulting PXRD patterns for the MCD apatite series indicate a lower crystallinity relative to the HA powder. The small peak present at  $31^\circ$  and  $34.4^\circ$  was attributed to the TCP phase [26]. Also in the MCD-425 pattern, peaks are poorly resolved with low intensity relative to the other apatites, demonstrating the more amorphous nature of this material [25,26].

**Figure 1.** Powder X-ray diffraction (PXRD) spectra of the powders (■ denotes HA peaks and \* represents tricalcium phosphate (TCP)).



The Fourier transform infrared spectrometer (FTIR) spectra of the powders in the range  $1600\text{--}450\text{ cm}^{-1}$  are presented in Figure 2. The most intense peaks observed for the crystalline HA powder are those attributable to vibrations of the  $\text{PO}_4^{3-}$  groups; the  $\nu_1$  and  $\nu_3$  phosphate bands in the region of  $900\text{--}1200\text{ cm}^{-1}$  and  $\nu_4$  absorption bands in the region of  $500\text{--}700\text{ cm}^{-1}$ , which are used to characterize apatite structure. The peak at  $962\text{ cm}^{-1}$  is assigned to the  $\nu_1$  symmetric P-O stretching vibration of the  $\text{PO}_4^{3-}$  and the  $\nu_3$  asymmetric P-O stretching mode are indexed at  $1090$  and  $1045\text{ cm}^{-1}$  [27]. The bands at  $601$  and  $571\text{ cm}^{-1}$  are assigned to  $\nu_4$  vibration mode of the phosphate group, which occupies two crystal lattice sites (O-P-O bending mode) according to previous studies [27]. The HA adsorption bands of the  $\nu_1$  and  $\nu_4$  of the  $\text{PO}_4^{3-}$  groups determined here are those of stoichiometric HA [16]. The bands at  $631$  and  $474\text{ cm}^{-1}$  correspond to the vibrations of  $\text{OH}^-$  groups in the structure [27]. The MCD series showed similar finger-print bonds for calcium phosphate bonds but with broader definition, which is representative of the increased amorphous content of these CaP materials [28].

**Figure 2.** Fourier transform infrared spectrometer (FTIR) spectra of the various apatite powders.

## 2.2. Characterization of the Modified Titanium Substrates

Titanium (V) was used as the base substrate and the untreated Ti surface was determined to contain 23% O and 77% Ti using EDX analysis. The chemical composition of the microblast surfaces (abrasive blast only, no dopant) are presented in Table 2 and were analyzed for O, Ca, P and Ti only.

**Table 2.** EDX analysis, coating thickness (PosiTector thickness gauge) and mass of the modified surfaces.

Modification		O % atm	P % atm	Ca % atm	Ti % atm	Ca/P	Coating Thickness ( $\mu\text{m}$ ) (2STD)	Coating Mass ( $\text{mg}/\text{cm}^2$ ) (2STD)
Blank	Ti	23	-	-	77	-	0	-
Microblast	MCD-106	59	8	12	21	1.56	$3 \pm 1$	-
	MCD-180	56	6	10	27	1.53	$3 \pm 1$	-
	MCD-425	55	7	11	27	1.57	$3 \pm 2$	-
CoBlast	HA/MCD-106	63	13	21	2	1.59	$6 \pm 3$	$0.48 \pm 0.4$
	HA/MCD-180	67	12	18	3	1.53	$6 \pm 1$	$0.44 \pm 0.4$
	HA/MCD-425	65	12	20	5	1.61	$7 \pm 3$	$0.44 \pm 0.3$

The % atm Ti determined reflects the exposure of the underlying substrate and can be used to represent the degree of coverage resulting from apatite materials. A high Ti level represents a thin or

patchy coating and conversely, a low Ti concentration signifies a thick coating. The EDX results reveal that after a wash treatment, the MCD microblasted surfaces show a reduction in Ti concentrations to 21–27% atm, compared to 77% atm for the Ti substrate. Also the presence of Ca and P which are the main constituents of the MCD abrasive is noted on the surface. This illustrates that a thin coating of Ca/P material has been blasted onto the surface and successfully deposited as a stable layer onto the Ti surface. The Ca/P values obtained for the microblasted samples treated with the MCD series of the abrasives ranged between 1.53 and 1.57 which is consistent with similar grit blasted studies [18].

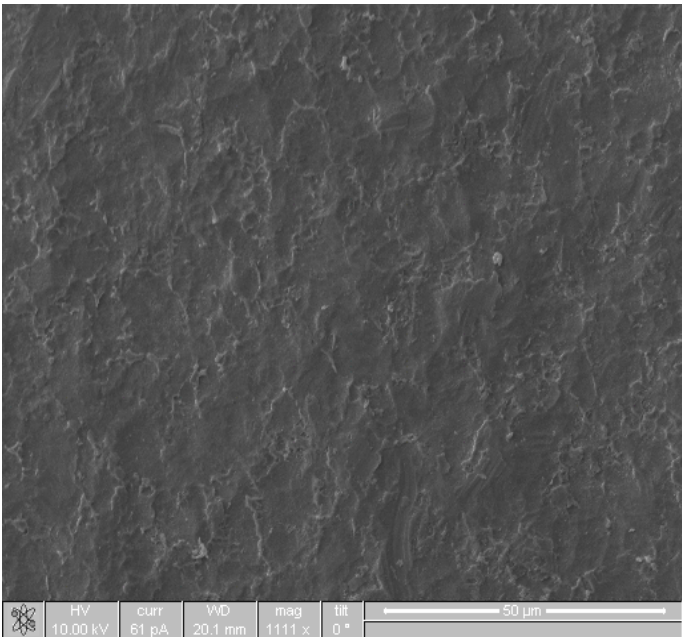
The chemical composition of the CoBlast surfaces (blasting with both abrasive and dopant) on Ti are also presented in Table 2. For CoBlast coatings, the levels of O, P, Ca and Ti obtained were determined to be in the range of 63–67%, 12–13%, 18–21% and 2–5% atm, respectively. The reduced level of Ti detected in these samples, compared to the Ti substrate and microblasted surfaces, is indicative of a high degree of coating coverage across all CoBlast samples. The Ca/P values were found to display a ratio of between 1.53 and 1.61, which are relatively close to the value for stoichiometric HA [25]. The % atm Ti, determined using EDX analysis, was observed to increase as the MCD series particle size order increased, indicating a decrease in the thickness of the deposited layer, as outlined in Table 2. This suggests that the smaller the particle size of the MCD abrasive the more HA was deposited, although the coating thickness determined using the PosiTector thickness gauge, and the coating mass values were found to be similar. The coating thickness of all the CoBlast samples was <10 microns which is in agreement with a previous study which used  $\text{Al}_2\text{O}_3$  as the abrasive [22].

The scanning electron microscopy (SEM) image of the untreated Ti substrate can be seen in Figure 3a which has similar topography to that observed in a previous study [6]. This image reveals a very smooth surface and the morphology of a machined metal. The SEM images of the microblast MCD-106 surfaces, as well as the corresponding CoBlast HA/MCD-106 surfaces, are presented in Figure 3b and c respectively. (More images can be seen as supporting information)

As expected, the microblast process was observed to roughen the untreated Ti surface. Examination of the CoBlast surfaces suggests that the co-introduction of the HA with the abrasive appears to have in-filled some of the surface features that are evident on the microblast sample (Figure 3b). The CoBlast process results in a roughened, highly regular and uniform surface which is consistent with other calcium phosphate coatings produced using simple grit blasting technologies [6,19,20]. It was noted that as the particle size ( $d_{90}$ ) of the MCD abrasive increased from 106 to 425 microns, the texture (presence of surface features) and the apparent roughness of the resultant surfaces was also observed to increase for both the microblast and CoBlast treatments and this was confirmed by surface roughness measurements.

**Figure 3.** Scanning electron microscopy (SEM) images ( $\times 1000$  magnification) of (a) titanium; (b) microblast MCD 106; (c) CoBlast HA/MCD-106.

(a)



(b)

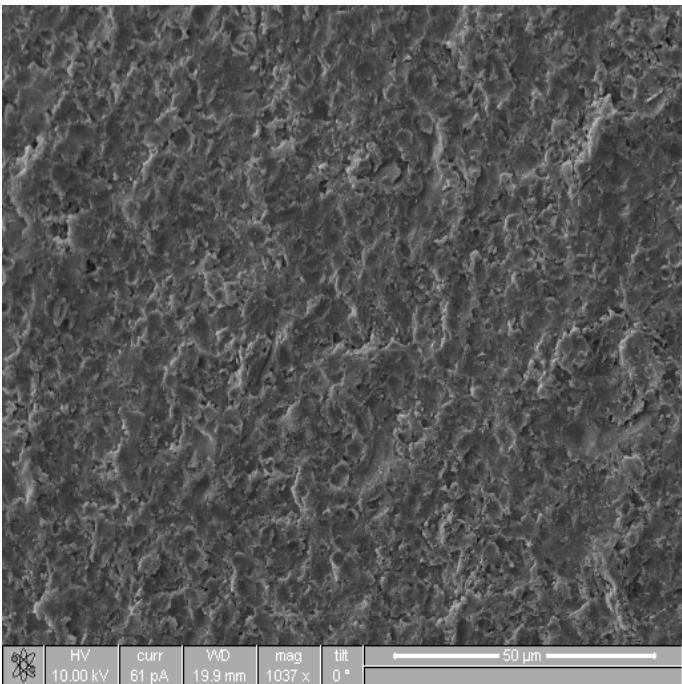
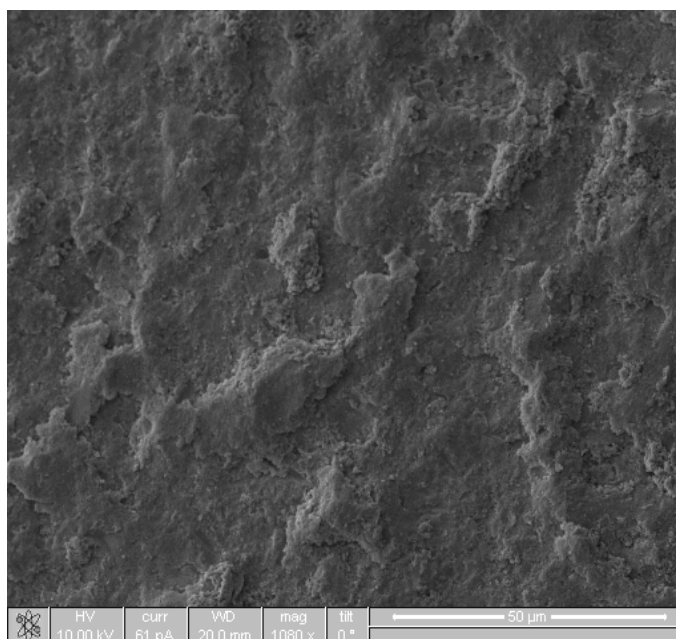




Figure 3. Cont.

(c)

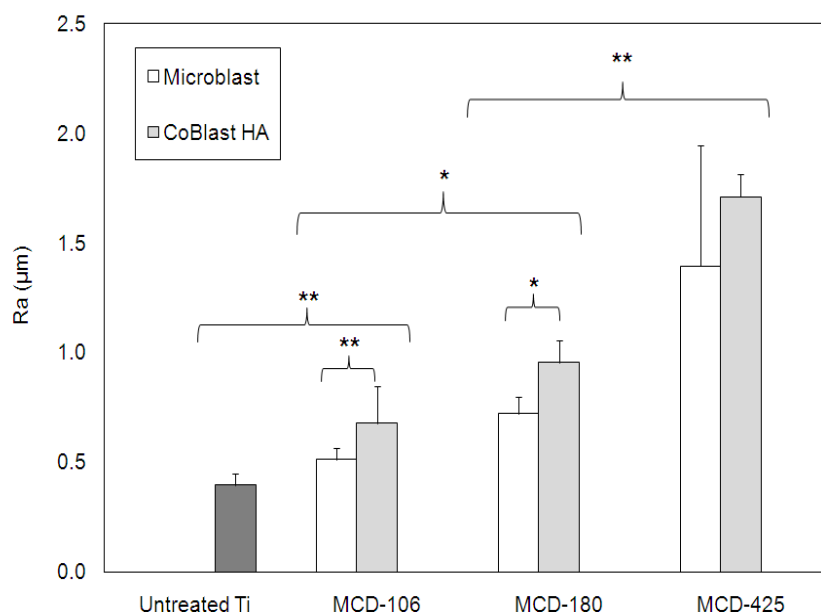


The surface roughness was measured using a stylus method and the results obtained are given in Figure 4. The arithmetical mean roughness ( $R_a$ ) was used as a measure of the surface roughness, which tended to increase as the particle size of the abrasive increased. Significant differences were observed between the surface treated and the untreated Ti. The average surface roughness of the blank titanium ( $0.4 \mu\text{m}$ ) increased to  $0.5$ ,  $0.8$ ,  $1.4 \mu\text{m}$  when MCD-106, MCD-180 and MCD-425, respectively were employed for microblast treatments. It has been previously reported that an increase in surface roughness was observed with the introduction of HA with the  $\text{Al}_2\text{O}_3$  abrasive using the CoBlast technique and the same trend was observed here on the introduction of HA with the MCD abrasives [21]. Statistically significant differences were noted between the roughness of the microblast and CoBlast samples prepared using MCD-106 and MCD-180 abrasives, though not when MCD-425 was used. A large standard error was observed for the MCD-425 microblasted surface, which may possibly be a feature of the crude microblast process. As per the microblast samples, the level of roughness and irregularity of the CoBlast surface was visibly altered by changes in the abrasive particle size, with a significant increase in surface roughness produced by larger abrasive particle sizes ( $p < 0.05$ ).

Implants with rougher surfaces result in a higher removal torque force and demonstrate excellent osteointegration when compared to those with smoother surfaces [5]. As seen in this study, microblasting offers increased roughening of machined Ti substrates as expected and the use of MCD abrasives results in the deposition of a thin coating layer of calcium phosphate. Furthermore, the roughness of the microblast process can be tuned between  $0.5$ – $1.4 \mu\text{m}$  depending on the particle size of the apatite abrasive employed. This is consistent with previously studies [5,6]. Unfortunately, the coatings deposited using this microblast process have demonstrated poor adhesion to the metal and have not been widely employed as final surface treatments for this reason [21].



**Figure 4.** Surface roughness ( $R_a$ ) of the various modifications (\* denotes  $p < 0.05$  and \*\* ascribes  $p < 0.01$  determined using student's t-test).



For the CoBlast samples, the tribo-chemical bonding which results from surface roughening, activation and subsequent bonding of the powder to the substrate has been shown to improve the HA bonding to the titanium [21,22]. The deposition of HA *via* the CoBlast process combines the benefits of increased roughness and enhanced bioceramic deposition with the added bioactive property of improved osteointegration compared to the microblasted surfaces. The surface treatment effect was also dependant on the particle size of the abrasive, with the larger particle size producing greater surface erosion and a rougher topography resulting in reduced coating thickness.

In literature, HA coatings, deposited using the standard high temperature plasma spray deposition technique, have been reported to contain a variety of crystalline phases and the presence of altered chemical functionality [9]. This can lead to the formation of intermediates such as calcium oxide (CaO), octa-hydroxyapatite (OHA),  $\alpha$ -tricalcium phosphate ( $\alpha$ -TCP),  $\beta$ -tricalcium phosphate ( $\beta$ -TCP) and tetra-calcium phosphate (TTCP) [10,11]. The presence of these impurities in a HA modified surface can decrease the crystallinity and subsequently make it more prone to dissolution. The increased solubility of these phases can eventually lead to the poor apposition of bone and compromise the mechanical stability of the implant [12, 29]. This can occur when the coating itself de-laminates over time due to poor bonding strength of the HA onto the underlying surface or as the coating itself resorbs into the surrounding environment [30].

Figure 5 shows the XRD pattern of the CoBlast HA coated substrates. Due to the thin nature of the deposited material and the interference of the background Ti metal, detailed analysis of the XRD profiles was not possible. However, for the CoBlast substrates, the peaks detected clearly correspond to that of HA powder employed. The additional  $2\theta$  peaks observed at  $35.3^\circ$  and  $38.5^\circ$  were assigned to the Ti substrate. No evidence of the TCP phase was detected ( $31^\circ$  and  $34.4^\circ$ ), which suggests that no compositional or crystallographic changes occurred to the HA powder during the blasting process, with negligible uptake of the abrasive, which is in keeping with previous studies [21,22].

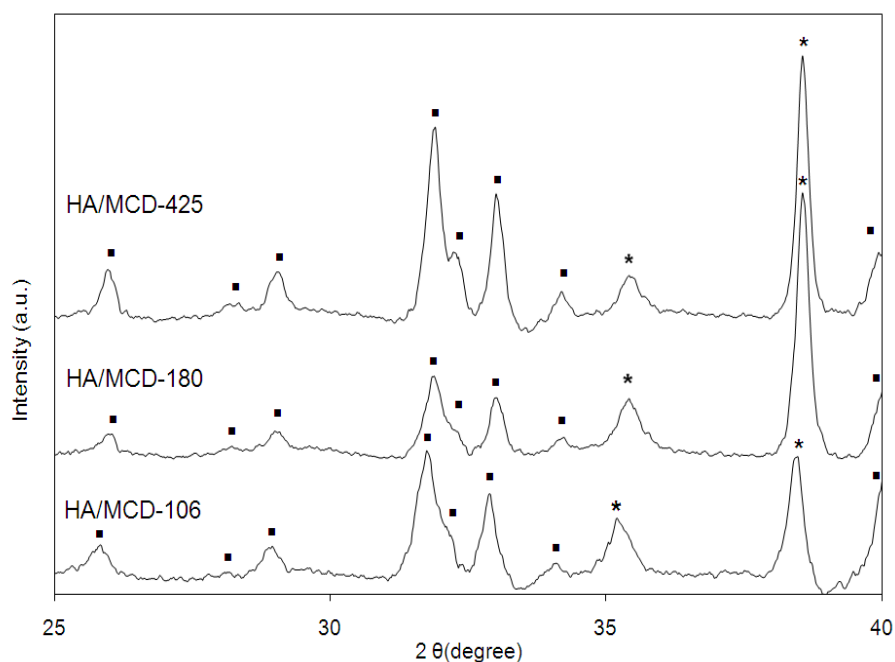
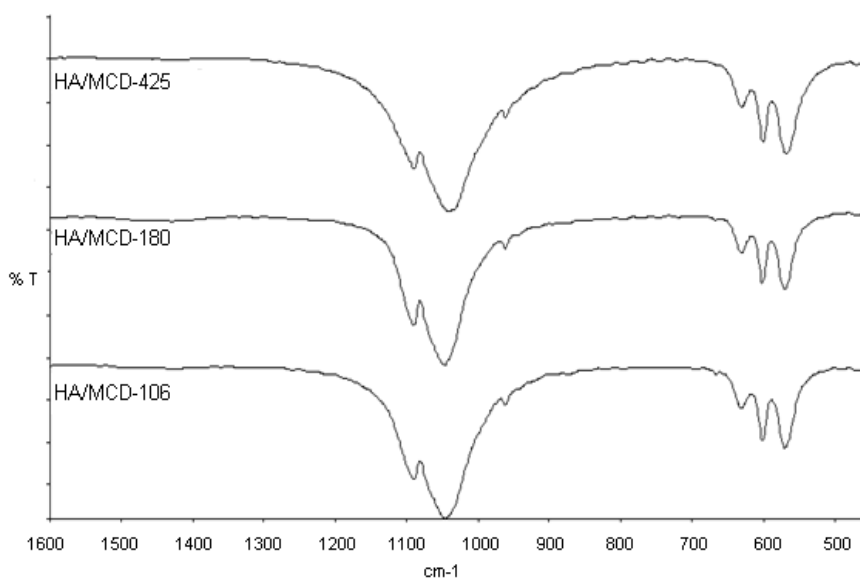
**Figure 5.** XRD of the CoBlast HA modifications (■ denotes HA peaks; \* denotes Ti peaks).

Figure 6 shows the FTIR spectrum in the range  $1600\text{--}450\text{ cm}^{-1}$  for the HA coated substrates. The FTIR spectra for all CoBlast HA coatings irrespective of the abrasive used are very similar and display the characteristic features of the HA powder used, as discussed earlier. There was no evidence of hydration (broad banding at  $3450\text{ cm}^{-1}$ ), further demonstrating a pure HA coating has been deposited. Also, the position of the characteristic peak at  $962\text{ cm}^{-1}$  represents a highly ordered, non-carbonated apatite and indicates a highly crystalline nature [16]. The banding assignments are in agreement with those of the HA powder as seen in Figure 2 suggesting that the chemistry is retained during the deposition process. This also supports the XRD analysis discussed above, which suggests that there has been minimal uptake of the abrasive powders during sample preparation.

**Figure 6.** FTIR analysis of the CoBlast HA surface modifications.

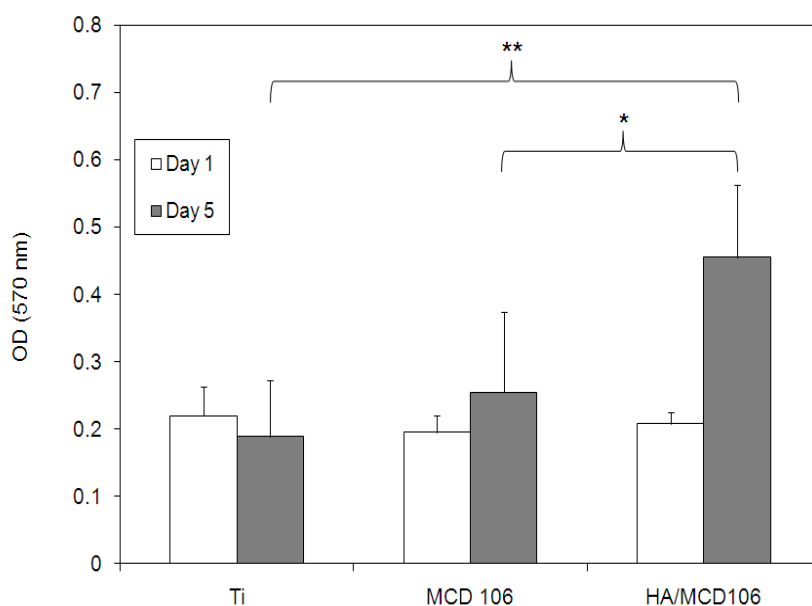
CoBlast demonstrated the ability to deposit a well adhered HA coating with no major evidence of contamination with additional calcium phosphate phases. This is in contrast to the variety of crystalline phases and the presence of altered chemical functionality produced during the standard high temperature plasma spray deposition. The XRD and FTIR analysis does not suggest formation of any such impurities within the CoBlast samples indicating that the HA coating on the CoBlast samples has retained the same properties as the starting crystalline HA powder employed. Therefore it is anticipated that HA modified surfaces prepared using CoBlast should not exhibit the problems associated with the presence of impurities observed for HA modified surfaces prepared using standard high temperature plasma spray which are outlined above.

### 2.3. Cell Culture Analysis

#### 2.3.1. Cell Proliferation

Osteoblasts are the key cells that are involved in the osteoconduction process. The success of the implantation is strongly influenced by how well the first phase of the attachment and adhesion of these cells will occur, which will then lead to the subsequent proliferation and differentiation upon contact with the implant surface. CoBlast surfaces have exhibited excellent osteoblast attachment and proliferation *in vitro* compared to their respective controls [21-23]. Biocompatibility of the modified surfaces was determined via a (3-(4,5-dimethylthiazol-2-yl)-2,5-diphenyltetrazolium bromide) (MTT) assay and the osteoblast proliferation results are presented in Figure 7.

**Figure 7.** (3-(4,5-dimethylthiazol-2-yl)-2,5-diphenyltetrazolium bromide) (MTT) assay data for MG-63 cells on modified Ti surfaces over five days *in vitro* (\* denotes  $p < 0.05$  and \*\* ascribes  $p < 0.01$  determined using student's t-test).



Microblast and CoBlast surfaces prepared using the MCD 106 abrasive were selected for comparison. There was no significant difference in the cell proliferation between samples analyzed at day 1. However, at day 5 there was a significant increase ( $p < 0.01$ ) in cell proliferation on the CoBlast coated substrate compared to the untreated titanium. A significant difference ( $p < 0.05$ ) was also detected between the CoBlast sample and the microblast sample at day 5. The introduction of the bioactive HA layer through the CoBlast process was shown to further increase surface roughness and this combination of surface topography and bioactive surface chemistry was found to offer notably higher levels of cell proliferation after 5 days on the CoBlast surface. No evidence of cytotoxicity was observed using MG63 cells on any of the samples evaluated. However, the surface coating thickness and surface roughness of the CoBlast coatings was found to be lower compared to plasma HA coating in literature (20–300  $\mu\text{m}$  thickness, 3–6  $\mu\text{m}$  Ra)[34] with increased cell proliferation observed on plasma HA compared to grit blasted surfaces [1].

### 2.3.2. Cell Morphology

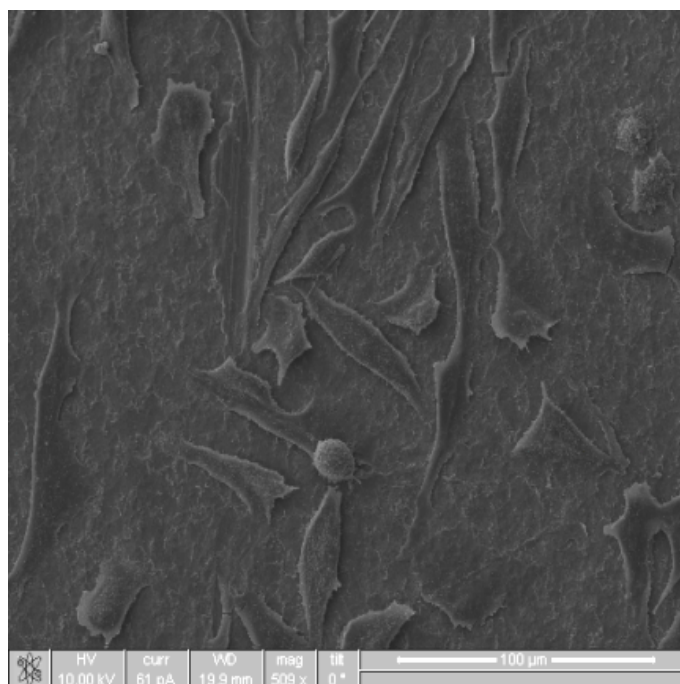
Surface modification techniques are extremely important for evoking desired cellular responses through tailoring the implants surface properties. The osteointegration process is greatly enhanced by these modifications, which in turn increases the long term success of the implant. As previously mentioned, HA is well known for its osteoconductive properties and its ability to influence cell adhesion and interaction at the implant-host interface. It is generally accepted that alongside chemical compatibility, the three dimensional surface topography (shape, size and surface texture) of the implant also influences early tissue response.

Figure 8 shows various images of MG63 cells that were cultured on the untreated titanium substrates, Figure 8a; microblasted MCD 106 surface, Figure 8b and CoBlast HA/MCD-106, Figure 8c after 24 hours.

Cells attached well to the untreated titanium surfaces and displayed a fibroblastic morphology synonymous with that of this osteoblastic cell line. The cells are typically polarized in one direction with the average cell length measuring roughly 60–80  $\mu\text{m}$  (Figure 8a). Furthermore, lamellopodia and filopodia extensions (cytoskeletal organisation) from the main body of cells onto the surface are observed. The presence of these processes suggest good cell-substrate interactions where the cell is actively probing for specific topographical features and connects the cell to the substrate (*via* filopodia) from the lamellopoda, which is the protrusion of their leading edge indicative of cell spreading and migration. However, the presence of numerous spherical cells indicates that not all cells are actively involved in spreading and migration. The cells cultured on MCD blasted surface (Figure 8b) display morphologies similar to that observed on the untreated titanium surfaces. The cells appeared to follow the contours of the MCD blasted surface where they would sit in the defects on the surface and align themselves along grooves or dents in a process referred to as ‘contact guidance’ [31]. The contact guidance effect has commonly been associated with increased cell proliferation and differentiation [31]. The surface roughness was determined to be 0.4, 0.5 and 0.7  $\mu\text{m}$  for the blank Ti, microblast MCD-106 and the CoBlast HA/MCD-106 respectively and this obviously influenced the proliferation results observed here as mentioned earlier.

**Figure 8.** MG-63 osteoblasts cultured on (a) untreated Ti and (b) microblasted MCD 106 treatment  $\times 500$  magnification and (c) HA/MCD-106 surfaces (CoBlast treatment) ( $\times 500$  magnification).

(a)



(b)

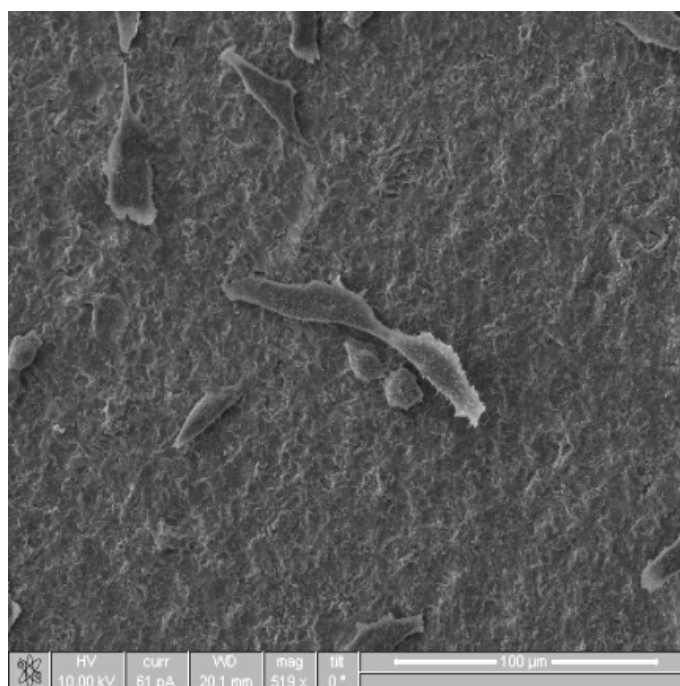


Figure 8. Cont.

(c)

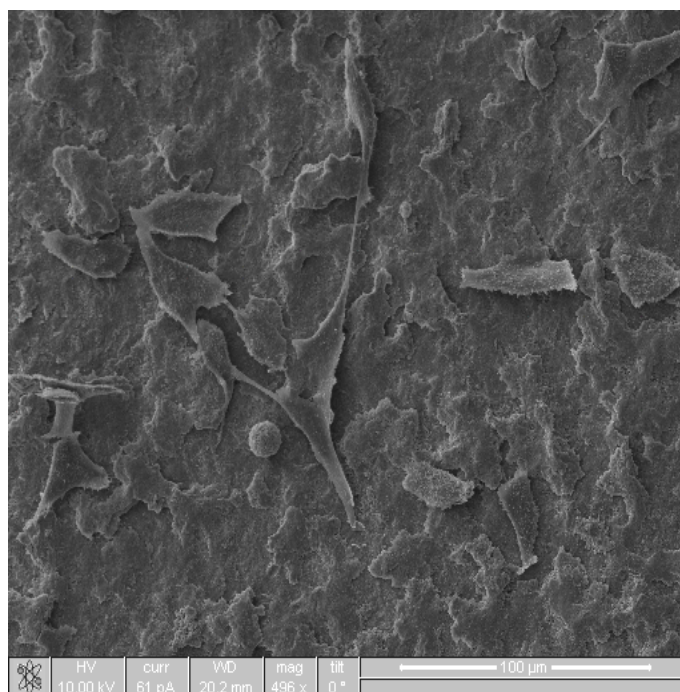


Figure 8c shows an image of MG-63 cells cultured on the CoBlast after 24 hours, it can be seen that these differed from those of the untreated and microblasted titanium in terms of morphology where they had a polygonal shape rather than a polarized fibroblastic morphology indicating increased cell spreading. The cells also tended to align to the surface features created by the addition of the bioactive layer, which was earlier observed to increase the surface roughness (Figure 4). An abundance of lamellopodia and filopodia were present on the CoBlast surface. The addition of a HA coat to the Ti surface, resulted in a higher order of cell spreading and cell focal adhesion attachment compared to the microblasted surface (Figure 8b).

Research has proven that the manufacturing process and patterned topography have a significant influence on long term adherence and cell proliferation *in vitro*, irrespective of composition and surface roughness [32] and early controlled osteoblast alignment was demonstrated on patterned substrates [33]. Therefore, due to the patterned nature of the HA surface after CoBlast treatment, a more favorable surface resulted for cell spreading which subsequently lead to increased cell viability compared to the microblast and blank Ti surfaces. *In vivo* evaluation of CoBlast substrates prepared using an alumina abrasive have already demonstrated early stage lamellar bone growth [21]. This study demonstrates that by employing differing grades of MCD abrasive in the CoBlast process, greater control over surface topography can be achieved, which offers the capability to improve bone-implant contact *in vivo*. Further *in vitro* evaluations such as dissolution studies and bioactive studies in stimulated body fluid (SBF) must be investigated to support these capabilities.

### 3. Experimental Section

#### 3.1. Materials

Titanium (Grade 5, Ti-6Al-4V) coupons (15 mm × 15 mm × 1 mm), were obtained from Lisnabrin Engineering Ireland. Hydroxyapatite [ $\text{Ca}_{10}(\text{PO}_4)_6(\text{OH})_2$ ] powder was sourced from S.A.I., France. The MCD apatite abrasives were all purchased from Himed Inc. (NY, USA). HPLC grade 1M hydrochloric acid (HCl), de-ionised water, isopropanol (IPA), ethanol, phosphate buffer solution (PBS), potassium bromide (KBr) FT-ir grade, Trypsin EDTA, MTT assay kit, ACS reagent grade dimethyl sulphoxide, paraformaldehyde, glutaraldehyde, osmium tetroxide and hexamethyldisilazane were all purchased from Sigma-Aldrich UK. MG-63 osteoblast cells were obtained from American Type Culture Collection, Rockville, MD, USA. Minimum Essential Medium (MEM), foetal calf serum, penicillin G sodium, streptomycin, amphotericin B were purchased from PAA Laboratories GmbH, Austria.

#### 3.2. Sample Preparation

Prior to surface modification, the coupons were cleaned ultrasonically in 1M HCl and then in isopropanol to remove any contaminants. The CoBlast technique was used to modify the titanium, through deposition with a HA layer. The processing utilized twin microblast nozzles for the dopant/abrasive system. The HA (dopant) was deposited onto the Ti coupons using compressed air at a pressure of 90 psi, speed of 13 mm/sec and a working distance of approximately 20 mm. The MCD abrasives (either MCD-106, MCD-180 or MCD-425) were blasted out of the second nozzle at a pressure of 75 psi and at a working distance of 8 mm from the surface. The microblast surfaces were prepared under the same corresponding conditions as above, however no HA was delivered through the dopant nozzle. After the surface treatment step, each sample was ultrasonically washed in de-ionized water for 5 mins to remove any loose powder from the surface.

#### 3.3. Surface Characterisation

The elemental composition of the powders and the coatings was carried out using a Jeol JSM 5510 SEM in conjunction with an INCA X-sight EDX spectroscopy detector (Oxford Instruments, Buckinghamshire, UK). Images were also taken using the same SEM system. Gravimetric analysis of the surface treatments on Ti was used to determine the coating mass using an Ohaus DV314C analytical balance by measuring the sample before and after an acid wash (ultrasonic treatment in 20 mL 1 M HCl for 10 mins). PXRD data was collected on a Siemens GAXRD diffractometer using  $\text{CuK}\alpha 1$  radiation, with an anode current of 30 mA and an accelerating voltage of 40 keV. Data was collected in the range of 20 to 60  $2\theta$  degrees with a step size of 0.02 and a scan rate of 1 s per step. Coating thickness was measured using a PosiTector 6000 N thickness gauge (DeFelsko, NY, USA). An average of six readings was used to determine each value. The surface roughness ( $R_a$ ) was determined using a Talsurf 10 surface profilometer (Talyor Hobson, UK). A Perkin Elmer Spectrum One FTIR was used to determine the structural fingerprint of the powders and the coatings. The coating was scrapped off, gently ground and pressed into a KBR disc (2% wt sample in KBR). Powders for FTIR analysis were prepared in a similar manner. FTIR spectra were recorded in the



1600–400-cm<sup>-1</sup> range, with 4 cm<sup>-1</sup> resolution using 20 scans and background subtraction. The spectra gave approximately 70–90% transmittance however the results are presented in an overlay fashion.

### 3.4. *In Vitro* Cell Culture

Sample modifications including CoBlast HA/MCD-106 and microblast MCD-106 and the blank Ti were evaluated for osteoconductivity and cytotoxicity using cell culture tests. Prior to cell culture analysis, each sample set was steam autoclaved at 121 °C for 20 minutes. MG-63 cells were used to assess cell proliferation. Cells were cultured in the MEM media supplemented with 10% foetal calf serum and antibiotic/antimycotic (penicillin G sodium 100 U/mL, streptomycin 100 µg/mL, amphotericin B 0.25 µg/mL) in 75 cm<sup>3</sup> tissue culture flasks. Cells were maintained in a humidified atmosphere with 5% CO<sub>2</sub> at 37 °C and were sub-cultured when they reached confluence using 0.25% Trypsin EDTA solution to provide adequate numbers of cells for the various *in vitro* culture studies undertaken.

#### 3.4.1. Cell Proliferation

MG-63 cell attachment to the various treated and untreated Ti substrates was determined after 4 hours in culture using a commercial MTT assay and employing a modified Mosmann method [24]. Cells were seeded onto the samples at a concentration of 1x10<sup>5</sup> cells/cm<sup>2</sup> and allowed to adhere during incubation at 37 °C in 5% CO<sub>2</sub> for 4 hrs. The MTT assay reagent was prepared as a 5 mg/mL stock solution in PBS, sterilized by filtration, and stored in the dark. An aliquot of the MTT stock solution (10% of total volume) was added to each well of a six well plate containing the samples (n = 4 for each sample type). After 3 hrs incubation at 37 °C in 5% CO<sub>2</sub>, 200 µl of dimethyl sulfoxide was added to dissolve the formazan crystals. The solution was agitated for 15 min on a shaker to ensure adequate dissolution. The optical density of the formazan solutions was read by spectrophotometry using an ELISA plate reader (Tecan Sunrise, Tecan Austria) at 570 nm with the background absorbance value measured at 650 nm. The absorbance values recorded were determined to be proportional to the number of cells attached to the surface in each case. All data reported are expressed as mean ± standard deviation.

#### 3.4.2. Cell Morphology

MG-63 cells were seeded onto each of the above substrates at a cell density of 5 × 10<sup>5</sup> cells/cm<sup>2</sup> in 6-well plates and were incubated for 24 hours. After cell culture, the samples were gently rinsed with PBS to remove any unattached cells and fixed in a modified Karnovsky's Fixative (2% paraformaldehyde/ 2% glutaraldehyde in PBS) for 1 hour. The samples were then rinsed in PBS and post-fixed in 1% osmium tetroxide and rinsed three times with PBS. The specimens were dehydrated by rinsing in an alcohol series (20, 30, 50, 70, 80, 90 and 95% ethanol), and finally rinsing 3 times in 100% ethanol. The samples were then chemically dried in hexamethyldisilazane (HMDS) overnight. A 50 nm layer of gold-palladium was deposited onto the substrates using a Polaron E5000 SEM Sputter Coating Unit. The sputtering conditions used a set voltage of 1.4 kV, with a plasma current of 18 mA (argon gas), a deposition time of 2 minutes at a vacuum pressure of 0.05 Torr. The

samples were then analyzed using the Jeol JSM 5510 SEM and subsequently using a FEI Quanta 200 Focused Ion Beam and SEM in backscatter electron mode.

#### 4. Conclusions

Detailed surface studies have shown that the combination of an apatite abrasive and a HA dopant in the CoBlast process produces surfaces with a combination of optimized apatite chemistry and controlled surface structure. The CoBlast process has the ability to retain the chemistry of the starting HA material. This offers advantages over conventional high temperature plasma processing which alters the HA material from its desired chemical, structural and dissolution requirements for its use as an *in vivo* implant material. The study also shows that employing MCD abrasives offer an alternative to alumina for deposition using CoBlast process. *In vitro* studies clearly show that increased roughness of treated surfaces favors enhanced cell proliferation and the CoBlast process offers the ability to tailor the surface texture to produce an optimized surface for osteointegration of a HA modified implant. Enhanced cell proliferation was observed for CoBlast modified surfaces compared to the microblasted surface. The ability of the CoBlast technology to offer diversity in modifying surface topography is clearly shown in this and previous studies and represents foundation work, which supported by bioactivity studies and *in vivo* trials, offers exciting new prospects in tailoring the properties of medical devices for applications ranging from dental to orthopedic settings.

#### Acknowledgments

The authors would like to acknowledge EnBio for supplying the CoBlast samples for this study.

#### References and Notes

1. Borsari, V.; Giavaresi, G.; Fini, M.; Torricelli, P.; Salito, A.; Chiesa, R.; Chiusoli, L.; Volpert, A.; Rimondini, L.; Giardino, R. Physical characterization of different-roughness titanium surfaces, with and without hydroxyapatite coating and their effect on human osteoblast-like cells. *J. Biomed. Mater. Res. Part B* **2005**, *75B*, 359-368.
2. Stoch, A.; Jastrze, B.W.; Dlugon, E.; Lejda, W.; Trybalska, B.; Stoch, G.J.; Adamczyk, A. Sol-gel derived hydroxyapatite coatings on titanium and its alloy Ti6Al4V. *J. Mol. Struct.* **2005**, *744*, 633-640.
3. Oh, I.H.; Nomura, N.; Chiba, A. Microstructures and bond strengths of plasma-sprayed hydroxyapatite coatings on porous titanium substrates. *J. Mater. Sci. Mater. Med.* **2005**, *16*, 635-640.
4. Lu, Y.P.; Li, M.S.; Li, S.T.; Wang, Z.G.; Zhu, R.F. Plasma-sprayed hydroxyapatite + titania composite bond coat for hydroxyapatite coating on titanium substrate. *Biomaterials* **2004**, *25*, 4393-4403.
5. Wennerberg, A.; Ektessabi, A.; Albrektsson, T.; Johansson, C.; Andersson, B.A. 1-year follow-up of implants of differing surface roughness placed in rabbit bone. *Inter. J. Oral Maxillofac. Implants* **1997**, *12*, 486-494.

6. Abron, A.; Hopfensperger, M.; Thompson, J.; Cooper, L.F. Evaluation of a predictive model for implant surface topography effects on early osseointegration in the rat tibia model. *J. Prosthet. Dent.* **2001**, *85*, 40-46.
7. Nakada, H.; Sakae, T.; Legeros, R.Z.; Legeros, J.P.; Suwa, T.; Numata, Y.; Kobayashi, K. Early tissue response to modified implant surfaces using back scattered imaging. *Implant Dent.* **2007**, *16*, 281-289.
8. Gil, F.J.; Planell, J.A.; Padros, A.; Aparicio, C. The effect of shot blasting and heat treatment on the fatigue behavior of titanium for dental implant applications. *Dent. Mater.* **2007**, *23*, 486-491.
9. Chen, J.; Wolke, J.G.C.; De Groot, K. Microstructure and crystallinity in hydroxyapatite coatings. *Biomaterials* **1994**, *15*, 396-399.
10. Gross, K.A.; Berndt, C.C.; Herman, H. Amorphous phase formation in plasma-sprayed hydroxyapatite coatings. *J. Biomed. Mater. Res.* **1998**, *39*, 407-414.
11. Gross, K.A.; Berndt, C.C. Thermal processing of hydroxyapatite for coating production. *J. Biomed. Mater. Res.* **1998**, *39*, 580-587.
12. Heimann, R.B.; Wirth, R. Formation and transformation of amorphous calcium phosphates on titanium alloy surfaces during atmospheric plasma spraying and their subsequent *in vitro* performance. *Biomaterials* **2006**, *27*, 823-831.
13. Weng, J.; Liu, Q.; Wolke, J.G.; Zhang, X.; De Groot, K. Formation and characteristics of the apatite layer on plasma-sprayed hydroxyapatite coatings in simulated body fluid. *Biomaterials* **1997**, *18*, 1027-1035.
14. Li, H.; Li, Z.X.; Li, H.; Wu, Y.Z.; Wei, Q. Characterization of plasma sprayed hydroxyapatite/ZrO<sub>2</sub> graded coating. *Mater. Design* **2009**, *30*, 3920-3924.
15. Katto, M.; Kurosawa, K.; Yokotani, A.; Kubodera, S.; Kameyama, A.; Higashiguchi, T.; Nakayama, T.; Tsukamoto, M. Poly-crystallized hydroxyapatite coating deposited by pulsed laser deposition method at room temperature. *Appl. Surf. Sci.* **2005**, *248*, 365-368.
16. Hong, Z.; Luan, L.; Paik, S.E.; Deng, B.; Ellis, D.E.; Ketterson, J.B.; Mello, A.; Eon, J.G.; Terra, J.; Rossi, A. Crystalline hydroxyapatite thin films produced at room temperature—An opposing radio frequency magnetron sputtering approach. *Thin Solid Films* **2007**, *515*, 6773-6780.
17. Stoch, A.; Brozek, A.; Kmita, G.; Stoch, J.; Jastrzebski, W.; Rakowska, A. Electrophoretic coating of hydroxyapatite on titanium implants. *J. Mole. Struct.* **2001**, *596*, 191-200.
18. Mano, T.; Ueyama, Y.; Ishikawa, K.; Matsumura, T.; Suzuki, K. Initial tissue response to a titanium implant coated with apatite at room temperature using a blast coating method. *Biomaterials* **2002**, *23*, 1931-1926.
19. Gbureck, U.; Masten, A.; Probst, J.; Thull, R. Tribochemical structuring and coating of implant metal surfaces with titanium oxide and hydroxyapatite layers. *Mater. Sci. Eng. C* **2003**, *23*, 461-465.
20. Ishikawa, K.; Miyamoto, Y.; Nagayama, M.; Asaoka, K. Blast coating method: New method of coating titanium surface with hydroxyapatite at room temperature. *J. Biomed. Mater. Res.* **1997**, *38*, 129-134.
21. O'Hare, P.; Meenan, B.J.B.; George, A.; Byrne, G.; Dowling, D.; Hunt, J.A. *In vitro* and *in vivo* response of hydroxyapatite surfaces deposited *via* a novel co-incident microblasting technique for improved orthopaedic implant performance. *Biomaterials* **2010**, *31*, 515-522.

22. O'Neill, L.; O'Sullivan, C.; O'Hare, P.; Sexton, L.; Keady, F.; O'Donoghue, J. Deposition of substituted apatites onto titanium surfaces using a novel blasting process. *Surf. Coat. Technol.* **2009**, *204*, 484-488.
23. O'Sullivan, C.; O'Hare, P.; O'Leary, N.D.; Crean, A.M.; Ryan, K.; Dobson, A.D.; O'Neill, L.D. Deposition of substituted apatites with anticolonizing properties onto titanium surfaces using a novel blasting process. *J. Biomed. Mater. Res. Part B* **2010**, *95*, 141-149.
24. Mosmann, T. Rapid colorimetric assay for cellular growth and survival: Application to proliferation and cytotoxicity assays. *J. Immunol. Methods* **1983**, *65*, 55-63.
25. Kim, T.N.; Feng, Q.L.; Kim, J.O.; Wu, J.; Wang, H.; Chen, G.C.; Cui, F.Z. Antimicrobial effects of metal ions ( $\text{Ag}^+$ ,  $\text{Cu}^{2+}$ ,  $\text{Zn}^{2+}$ ) in hydroxyapatite. *J. Mater. Sci.: Mater. Med.* **1998**, *9*, 129-134.
26. Fathi, M.H.; Hanifi, A.; Mortazavi, V. Preparation and bioactivity evaluation of bone-like hydroxyapatite nanopowder. *J. Mater. Proc. Technol.* **2008**, *202*, 536-542.
27. Varma, H.K.; Babu, S.S. Synthesis of calcium phosphate bioceramics by citrate gel pyrolysis method. *Ceram. Int.* **2005**, *31*, 109-114.
28. Pleshko, N.; Boskey, A.; Mendelsohn, R. Novel infrared spectroscopic method for the determination of crystallinity of hydroxyapatite minerals. *Biophys. J.* **1991**, *60*, 786-793.
29. Legeros, R.Z.; Daculsi, G.; Orly, I.; Gregoire, M. Substrate surface dissolution and interfacial biological minerals. In *The Bone-Biomaterial Interface*; Davies, J.E., Ed.; University of Toronto: Toronto, Canada, 1991; pp. 76-88.
30. Masmoudi, M.; Assoul, M.; Wery, M.; Abdelhedi, R.; El Halouani, F.; Monteil, G. Friction and wear behaviour of cp Ti and Ti6Al4V following nitric acid passivation. *Appl. Surf. Sci.* **2006**, *253*, 237-2243.
31. Anselme, K. Osteoblast adhesion on biomaterials. *Biomaterials* **2000**, *21*, 667-681.
32. Bigerelle, M.; Anselme, K. Statistical correlation between cell adhesion and proliferation on biocompatible metallic materials. *J. Biomed. Mater. Res. A* **2005**, *75*, 530-540.
33. Puckett, A.; Pareta, R.; Webster, T.J. Nano rough micron patterned titanium for directing osteoblast morphology and adhesion. *Inter. J. Nanomed.* **2008**, *2*, 229-241.
34. Sun, L.; Berndt, C.C.; Gross, K.A.; Kucuk, A. Material fundamentals and clinical performance of plasma-sprayed hydroxyapatite coatings: A review. *J. Biomed. Mater. Res.* **2001**, *58*, 570-592.